Bull Earthquake Eng (2009) 7:391–410
DOI 10.1007/s10518-008-9069-2

ORIGINAL RESEARCH PAPER

Direct displacement-based design of seismically isolated bridges

D. Cardone · M. Dolce · G. Palermo

Received: 29 December 2007 / Accepted: 2 May 2008 / Published online: 3 July 2008

Abstract A Displacement-Based Design (DBD) procedure for bridges equipped with different seismic Isolation Systems (IS's) is proposed. It has been derived from the Direct DBD method recently developed by Priestley and co-workers. The key aspect of the proposed procedure is the definition of a uniform target displacement of the deck, which is assigned by the designer to accomplish a given performance level, expressed through limit values of the maximum IS displacement and of the pier drift, respectively. The proposed design procedure has been developed for four different idealized force-displacement cyclic behaviours of IS's, which can be used to describe the response of a wide variety of IS's, including: (i) Lead-Rubber Bearings (LRB), (ii) High-Damping Rubber Bearings (HDRB), (iii) Friction Pendulum Bearings (FPB), (iv) Combinations of either Low-Damping Rubber Bearings (LDRB) or FPB and Viscous Dampers (VD), (v) Combinations of lubricated Flat Sliding Bearings (FSB) and LDRB, (vi) Combinations of FSB and Steel Yielding Devices (SYD), (vii) Combinations of FSB, Shape Memory Alloy (SMA)-based Re-centring Devices and VD. In the paper, the background and implementation of the design procedure is presented first, then some validation studies through nonlinear time-history analyses on different configurations of continuous deck and multi-span simply supported deck bridges are illustrated.

Keywords Bridges · Seismic isolation systems · Displacement-based design · Displacement response spectra · Equivalent viscous damping

1 Introduction

It is widely recognized that the traditional force-based design approach cannot provide the appropriate means for implementing concepts of Performance-based Earthquake

D. Cardone (✉) · G. Palermo
DiSGG, University of Basilicata, Macchia Romana Campus, 85100 Potenza, Italy
e-mail: donatello.cardone@unibas.it

M. Dolce
Italian Department of Civil Protection, via Vitorchiano 4, 00189 Rome, Italy

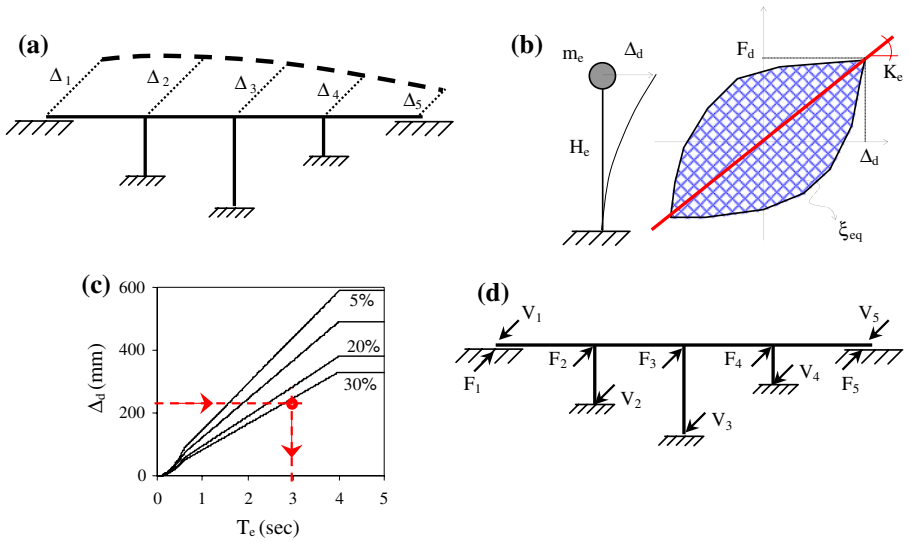

Fig. 1 Fundamentals of DDBD, with specific reference to bridge structures

Engineering (Bertero and Bertero 2002). Performance levels, indeed, are described in terms of displacements, as damage is better correlated to displacements rather than forces. As a consequence, new design approaches, based on displacements, have been recently implemented. One of such approach is the Direct Displacement-Based Design (DDBD), proposed by Priestley (1993). The fundamental goal of DDBD is to obtain a structure which will reach a target displacement profile when subjected to earthquakes consistent with a given reference response spectrum.

Figure 1 shows the fundamental steps in the application of DDBD for bridges. The first two steps (Fig. 1a, b) highlight the most important differences between DDBD and force-based seismic design.

Force-based design characterizes the structure through its elastic properties (initial stiffness and elastic damping). The maximum acceleration response of the elastic structure is determined from response spectrum analysis. It is then reduced by a behaviour modification factor (q in the Eurocode 8 (CEN 1998)) to obtain the design acceleration profile, hence design lateral forces for the resistance verifications at the ultimate limit state. Displacements are only checked at the end of the design process, usually to satisfy service requirements at the damage limit state.

In the DDBD, the nonlinear MDOF model of the structure is replaced by an equivalent linear SDOF system (Substitute Structure Approach firstly proposed by (Shibata and Sozen 1976)), whose properties (K_e and ξ_{eq}) correspond to the effective lateral stiffness and equivalent viscous damping of the real structure at the peak displacement response.

The target displacement profile Δ_i is set by the designer at the beginning of the procedure, to ensure specified performance levels for a given level of seismic excitation.

The substitute structure will present a design force (F_d) corresponding to the maximum base shear of the real structure and an equivalent design displacement (Δ_d) corresponding to the assigned target displacement profile of the deck (see Fig. 1a). The design displacement Δ_d can be obtained using the following equation (Priestley 2003):

$$\Delta_d = \frac{\sum_{i=1}^{n} \left(m_i \cdot \Delta_i^2\right)}{\sum_{i=1}^{n} \left(m_i \cdot \Delta_i\right)} \tag{1}$$

where n is the number of piers/abutments, m_i is the appropriate contribution of deck (and pier) mass at each pier/abutment location and Δ_i is the corresponding deck displacement.

The equivalent damping of the SDOF system accounts for the energy dissipated by the real structure during the seismic excitation through its viscous, frictional and hysteretic behaviour. It is computed based on either analytical formulations or semi-empirical relationships, as a function of the displacement or ductility demand of the system.

Since the equivalent properties of the substitute structure are elastic, a set of elastic displacement response spectra is used to determine the effective period T_e associated to the design displacement Δ_d and corresponding damping ratio (Fig. 1c). The effective stiffness of the equivalent SDOF system (K_e) is found by inverting the well-known relationship:

$$K_e = 4\pi^2 \cdot m_e / T_e^2 \tag{2}$$

where m_e is the effective mass of the substitute structure, which can be expressed as a function of the target displacement profile (Priestley 2003):

$$m_e = \frac{\sum_{i=1}^{n} \left(m_i \cdot \Delta_i\right)}{\Delta_d} \tag{3}$$

Finally, the design base shear is computed ($V_b = F_d = K_e \cdot \Delta_d$) and then distributed as inertial forces to each mass location (see Fig. 1d):

$$F_i = V_b \cdot \frac{m_i \cdot \Delta_i}{\sum_{i=1}^{n} \left(m_i \cdot \Delta_i\right)} \tag{4}$$

The DDBD method has been recently specialized to different structural types, including frame buildings (Pettiga and Priestley 2005), wall buildings (Sullivan et al. 2005) and continuous deck bridges (Kowalsky 2002).

An early displacement-based approach for the design of bridges with seismic isolation can be found in (Priestley et al. 1996; Calvi and Pavese 1997). Recently Priestley et al. (2007) proposed the extension of the DDBD method to bridges with seismic isolation. In this paper, the DDBD method for bridges with seismic isolation is fully developed for different types of Isolation Systems (IS's) and implemented in MATLAB through an automatic iterative procedure.

The IS types taken into account include: (1) High Damping Rubber Bearings (HDRB), (2) Lead Rubber Bearings (LRB), (3) Friction Pendulum Bearings (FPB) and (4) combinations of Flat Sliding Bearings (FSB) with different auxiliary devices. As far as the bridge configuration is concerned, the proposed methodology can be applied to multi-span both continuous deck and simply supported deck bridges with piers of different heights.

The key aspect of the design method is the target displacement profile of the deck. It is specified by assigning a suitable displacement pattern and a target displacement amplitude to the deck. The target displacement amplitude, in particular, is selected by the designer to comply with a given performance level, expressed in terms of a limit value of the maximum IS displacement and pier drift. Going through a rapidly converging iteration process, the proposed design procedure provides the basic mechanical properties of each IS and pier reinforcement that realize the required performance level.

In the following paragraphs the basic modeling assumptions of the method are presented first and the design algorithm is then described, considering separately the design of new

bridges and the retrofitting of the existing ones. Finally, the results of some validation studies, conducted with nonlinear time-history analysis, are reported.

2 Design procedure

2.1 Design performance objectives

The design philosophy of the proposed procedure is based on the general requirement that the full serviceability of the bridge should be maintained after the design seismic event, so that there should be no need to reduce traffic over the bridge nor to carry out any repairs. In order to satisfy the above said general requirement, the design must comply with the following criteria: (i) the seismic response of the superstructure (deck, movement joints, restrainers) and substructures (piers, abutments, foundations) must remain essentially elastic, (ii) due to the critical role of its displacement capacity for the safety of the entire structure, the IS must be able to sustain a maximum horizontal displacement greater than that generated by the design earthquake, (iii) adequate clearance should be provided to the movement joints, in order to accommodate the IS displacements, in both longitudinal and transverse direction, thus avoiding impacts between structural elements or damage to movement joints.

The design displacement of the IS in each direction is assigned by the designer based on preliminary considerations (see below), taking into account the IS type selected. The maximum pier displacements and the maximum relative displacements between adjacent structural members at the movement joints are iteratively checked during the design process, in order to finally get lower values than the corresponding yield displacements and available clearances, respectively.

The use of seismic isolation as seismic protection technique allows for an additional design assumption: a bridge response in the transverse direction characterized by a rigid translation of the deck. In most cases, indeed, the deformation of the deck in its horizontal plane is negligible compared to the displacements of the pier-IS systems. At the beginning of the seismic design process, moreover, pier geometry (including pier height and cross section dimensions) is usually known, as it results from geographical and architectural constraints, as well as non-seismic load conditions. The IS's can be then purposely designed to get the coincidence between the centre of stiffness of the pier-IS systems and the centre of mass of the supported deck. In this way, torsional effects in the piers are eliminated and relative rotations at the movement joints avoided, as far as asynchronous ground motions are not considered. The aforesaid assumption gives also the advantage of greatly simplify the design formulas of the DDBD method (see Eqs. 1, 3 and 4), which reduce to: $\Delta_d = \Delta_i$, $m_e = \sum_{i=1}^{n} (m_i)$ and $F_i = V_b \cdot m_i / \sum_{i=1}^{n} (m_i)$, respectively.

For multi-span simply supported deck bridges, two different models of analysis are considered. In the transverse direction, the pier-deck connections are supposed to be fully effective in constraining the relative transverse movements between adjacent spans. As a consequence, the DDBD method is applied to the bridge as a whole. In the longitudinal direction, on the contrary, the joints are supposed free to move. As a consequence, the analysis is carried out on independent stand-alone spans, considered as completely separated from the adjacent spans at the movement joints.

In the current version of the method, the IS characteristics in the transverse direction of the bridge are first defined. The IS characteristics in the longitudinal direction are then adjusted to achieve the corresponding performance objective, taking into account the (possible) different behaviour of the piers. Unidirectional Sliding Pot-Bearings (Eggert and Kauschke 2002),

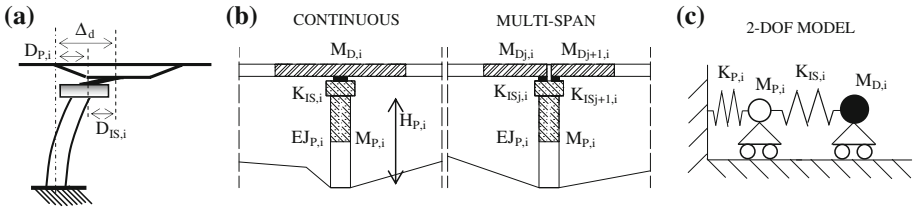

Fig. 2 (**a**) Deformed shape of the i-th pier-IS-deck system in the transverse direction, (**b**) contributing pier mass and tributary deck mass(es) for continuous and multi-span bridges, (**c**) simplified 2-DOF model for the evaluation of the effective mass of each pier-IS-deck system

placed on the top of a number of isolation devices (HDRB, LRB, FPB, etc.), are supposed to be used in order to get, for each IS, the required mechanical behaviour in the longitudinal and transverse direction.

2.2 Numerical model for continuous and multi-span simply supported deck bridges

The proposed design procedure is addressed to multi-span both continuous and simply supported deck bridges. It is based on an equivalent linear SDOF model of the bridge (see Fig. 1b), which is derived from the examination of each pier-IS-deck system. Figure 2a shows the deformed shape of the i-th pier-IS-deck system at the peak seismic response of the bridge in the transverse direction. In Fig. 2a, Δ_d represents the assumed target displacement of the deck, which is the same for each pier-IS-deck system, $D_{P,i}$ the fraction of Δ_d absorbed by the pier and $D_{IS,i}$ the complementary part that should be accommodated by the IS. The displacements $D_{P,i}$ and $D_{IS,i}$ change from one pier-IS-deck system to another, but their sum is always the same (Δ_d).

Figure 2b shows the tributary deck mass and the contributing pier mass considered for each pier-IS-deck system. The contributing pier mass ($M_{P,i}$ in Fig. 2c) is computed as the sum of the mass of the pier cap and one third of the pier mass. It is lumped at the top of the pier. For continuous bridges, the tributary deck mass ($M_{D,i}$ in Fig. 2c) is simply taken equal to the mass of half span on the left and half span on the right. The same holds for multi-span bridges in the transverse direction, due the constraining action of the joints. Obviously, also the effective stiffness values of the IS's placed on the same pier are summed. In the longitudinal direction, on the contrary, two independent pier-IS-deck systems, sharing the same pier while differing in the tributary deck mass ($M_{Dj,i}$ and $M_{Dj+1,i}$ in Fig. 2b) and IS effective stiffness ($K_{ISj,i}$ and $K_{ISj+1,i}$ in Fig. 2b), are considered.

The evaluation of the first-mode participating mass of the 2-DOF systems thus defined (see Fig. 2c) provides the effective masses of each pier-IS system (m_i^*), to be used in Eqs. 1–4, which govern the DDBD method.

2.3 Modeling of isolation systems

In the proposed design procedure four different force-displacement models have been considered to describe the IS cyclic behaviour. They are shown in Fig. 3, with the associated model parameters. The first model (see Fig. 3a) represents a visco-elastic behaviour. It can be used to describe the behaviour of HDRB (Derham et al. 1985) and LDRB (Taylor et al. 1992). The second model (see Fig. 3b) represents an elasto-plastic with hardening behaviour. It can be used for HDRB, LRB (Kelly 1992) and Steel Yielding Devices (SYD). The third model (Fig. 3c) represents a rigid-plastic with hardening behaviour, which can be exploited to describe FPB (Al-Hussaini et al. 1994) or combinations of FSB and LDRB. The

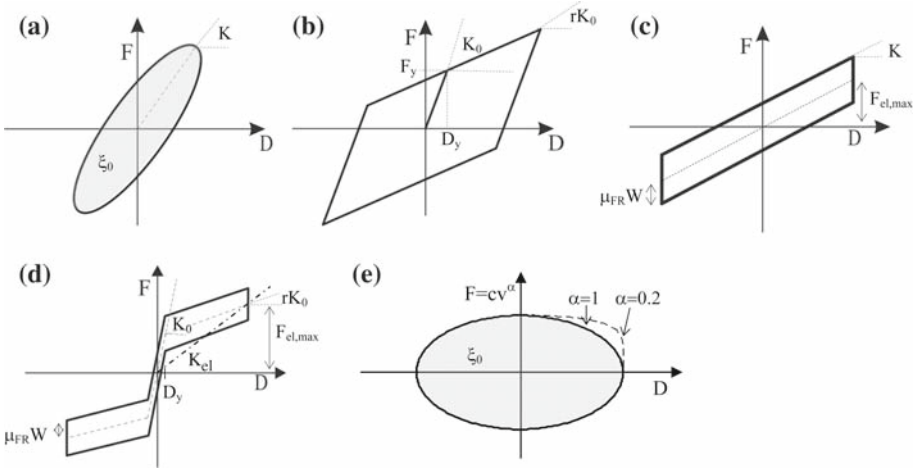

Fig. 3 Schematic behaviour of IS's and auxiliary viscous dampers: (**a**) Visco-Elastic; (**b**) Elasto-Plastic with hardening; (**c**) Rigid-Plastic with hardening; (**d**) Double-Flag-shaped; (**e**) Linear ($\alpha = 1$) and strongly nonlinear ($\alpha = 0.2-0.3$) viscous models

forth model (referred to as double flag-shaped model, see Fig. 3d) derives from the combination of a bilinear nonlinear elastic behaviour, modeling the typical F-d cycles of SMA-based re-centring devices (Dolce et al. 2000), and a rigid-plastic behaviour, reproducing the schematic F-d cycles of FSB (Dolce et al. 2005). Linear ($\alpha = 1$) or nonlinear ($1 < \alpha < 0.2$–0.3) viscous models (Fig. 3e) are used to take into account possible auxiliary viscous dampers (Constantinou et al. 1993).

The models shown in Fig. 3a and 3e correspond to velocity-dependent IS devices/systems, for which the viscous damping ratio can be selected as design parameter at the beginning of the analysis.

The models of Fig. 3b–3d refer to displacement-dependent IS's, for which the effective damping ratio is computed based on the maximum displacement response of the IS. In this case, a number of iterations are needed, as damping ratio and maximum displacement response of the IS are mutually related. In the proposed procedure, the effective damping ratio of displacement-dependent IS's is calculated based on the well-known Jacobsen's equation (Chopra 1997):

$$\xi_{IS} = \frac{W_{\mathrm{d}}}{4\pi \cdot W_{\mathrm{s}}} = \frac{W_{\mathrm{hysteresis}} + W_{\mathrm{friction}}}{2\pi \cdot F_{\mathrm{IS}} \cdot D_{\mathrm{IS}}} \tag{5}$$

in which W_{d} is the total energy dissipated by the IS in the cycle of maximum amplitude, W_{s} the strain energy stored at the maximum displacement D_{IS} and F_{IS} the force in the IS at the maximum displacement.

The aforesaid general expression of the equivalent damping ratio can be particularized to each IS, making use of its basic mechanical parameters. The specification of practical values for such basic mechanical parameters is fundamental both for helping the designer in the selection of the model parameters at the beginning of the analysis and for evaluating typical values of damping ratio for each IS.

In Fig. 4, the effective damping ratio of IS's responding according to an elasto-plastic with hardening model (e.g. LRB, HDRB, SYD), a rigid-plastic with hardening model (e.g. FPB) and a double flag-shaped model (e.g. SMA+FSB) are reported. As can be seen, the effective

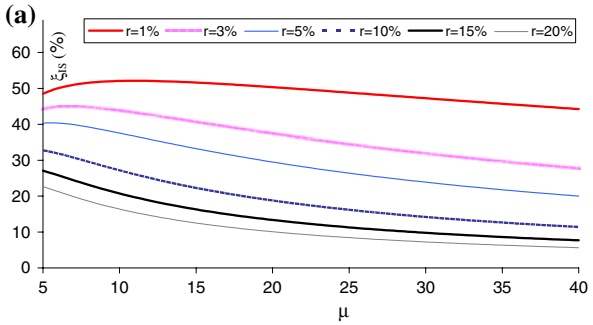

$$\xi_{IS} = \frac{2(\mu-1)(1-r)}{\pi\mu(1+r(\mu-1))}$$

	HDRB	LRB	SYD
μ	<15	<40	var.
r	$15-25\%$	$5-15\%$	$1-5\%$
ξ_{IS}	$15-25\%$	$20-30\%$	$>30\%$

$$\xi_{IS} = \frac{2}{\pi(1+\Lambda)}$$

FPB	SMA+FSB
$\Lambda = \frac{D}{R\mu_{FR}}$	$\Lambda = \frac{4D}{\mu_{FR}T_{el}^2}$
$\frac{D}{R} \cong 7.5-15\%$ $\mu_{FR} \cong 2-5\%$	$\mu < 50$ $r \cong 5-10\%$ $\mu_{FR} \cong 2-5\%$
$\Lambda \cong 1.5-7.5$	$\Lambda \cong 1.3-10$
$\xi_{IS} \cong 7.5-25\%$	$\xi_{IS} \cong 5-27\%$

Fig. 4 Typical mechanical parameters and damping ratios of currently used IS's

viscous damping of elasto-plastic with hardening IS's (see Fig. 4a) depends on two main parameters: the post-yield hardening ratio r and the displacement ductility μ. The effective damping reduces while increasing the displacement ductility and the hardening ratio. Typical values of displacement ductility and hardening ratio, usually adopted for three noteworthy IS's responding according to an elasto-plastic model, are reported in the table on the right hand side of Fig. 4a. They have been derived by examining different sources on this topic (Naeim and Kelly 1999; Skinner et al. 1993; Higashino and Okamoto 2006). The associated ranges of effective damping are pointed out in the last row of the table. As can be seen, HDRB exhibits damping ratios ranging from 15% to 25% while LRB from 20% to 30%. The effective damping ratio of SYD surely exceeds 30%, according to the Jacobsen's approach (see Eq. 5). Actually, recent studies by Priestley et al. (2007) show that relatively large reduction factors should be applied to the area-based damping (ref. Eq. 5) of elasto-plastic systems with low post-yield hardening ratios, in order to get an effective viscous damping consistent with the effective stiffness idealization of the system adopted within the DDBD method. The results by Priestley et al. (2007), however, cannot be extended to this study, basically because they refer to ductility values too low for IS systems. Further analyses are then needed to derive suitable correction factors to the area-based effective damping of SYD.

The effective damping of rigid-plastic with hardening and double flag-shaped IS's (see Fig. 4b) can be expressed as a function of the parameter Λ, defined as the ratio between the maximum restoring force of the IS ($F_{\mathrm{el,max}}$ in Fig. 3) and the friction resistance ($F_{\mathrm{FR}} = \mu_{\mathrm{FR}} * W$ in Fig. 3) of the sliding bearing, μ_{FR} being the dynamic friction coefficient and W the normal load sustained by the sliding bearing.

For FPB systems, in particular, Λ can be conveniently rewritten as the ratio between the maximum expected horizontal displacement (D) and the product between the radius of curvature of the slider (R) and its friction coefficient (μ_{FR}), as indicated in the table on the right-hand side of Fig. 4b. Sliding bearings (with or w/o curved surfaces) used in seismic isolation typically exploit the low friction coefficient (typically of the order of 2–5% (Dolce et al. 2005)) between pads of PTFE or other special materials in contact with lubricated polished stainless steel surfaces. The ratio between the maximum horizontal displacement and the radius of curvature of FPB is generally limited between 7.5% and 15% (see Priestley et al. (2007)), in order to rely upon an adequate re-centring capacity while avoiding excessive vertical displacements. As a result, for FPB, Λ can vary approximately between $1.5(\Lambda_{\min} = (D/R)_{\min}/\mu_{FR,MAX} = 7.5/5 = 1.5)$ and $7.5(\Lambda_{MAX} = (D/R)_{MAX}/\mu_{FR,\min} = 15/2 = 7.5)$ and the corresponding effective damping ratios between 7.5% and 25% (see Fig. 4b). With the addition of a purely viscous element (Fig. 3e), the damping capacity of FPB+VD or FSB+LDRB isolation systems can be captured.

For SMA+FSB systems, Λ can be conveniently expressed as a function of the design horizontal displacement (D) and period of vibration T_{el} (see Fig. 3d) of the isolated structure, as indicated in the table on the right-hand side of Fig. 4b. Referring to the typical values of design displacement (0.15–0.25 m) and period of vibration (2–3 s) of structures with SMA-based isolation systems (Dolce et al. 2007), effective damping ratios ranging from 5% to approximately 27% ($\Lambda \approx 1.33 - 10$) are found.

2.4 Design algorithm

The main goal of the design is to define the IS characteristics that permit to satisfy the performance objective stated before, i.e. realizing a bridge which responds according to a given target displacement profile when subjected to the design seismic event. The target displacement profile is specified by assigning to the deck a uniform displacement pattern, characterized by a suitable design displacement amplitude. The design displacement amplitude results from a combination of pier and IS displacements. The design pier displacements are essentially governed by the assumption of maintaining piers elastic. Therefore, reference is made to their yield displacements, properly reduced to take into account possible overstrength of the IS's. The IS design displacement is derived from considerations related to the IS displacement capacity and/or from the available clearances at the movement joints. Obviously, the two contributions to the deck design displacements change from one pier-IS-deck system to another and from longitudinal to transverse direction. The third key aspect of the design (besides IS and pier displacements) is pier reinforcement. When dealing with the seismic retrofit of existing bridges, the pier reinforcement is known. When dealing with the seismic design of new bridges, a preliminary design of the bridge has been already performed, based on non-seismic load conditions. The full geometry of the piers and a preliminary dimensioning of their reinforcement are therefore already available.

In any case, a preliminary careful selection of IS type (with associated mechanical parameters), design displacement and pier reinforcement ratio is strongly recommended. This can be done with the graphical procedure shown in Fig. 5a, for existing bridges, and in Fig. 5b, for new bridges.

In Fig. 5, there are reported a number of high-damping elastic spectra in the so-called ADRS (Acceleration-Displacement-Response-Spectra) format. Basically, each IS type is characterized by a different damping level (see Fig. 4). As a consequence, each IS type can be associated to a different group of response spectra.

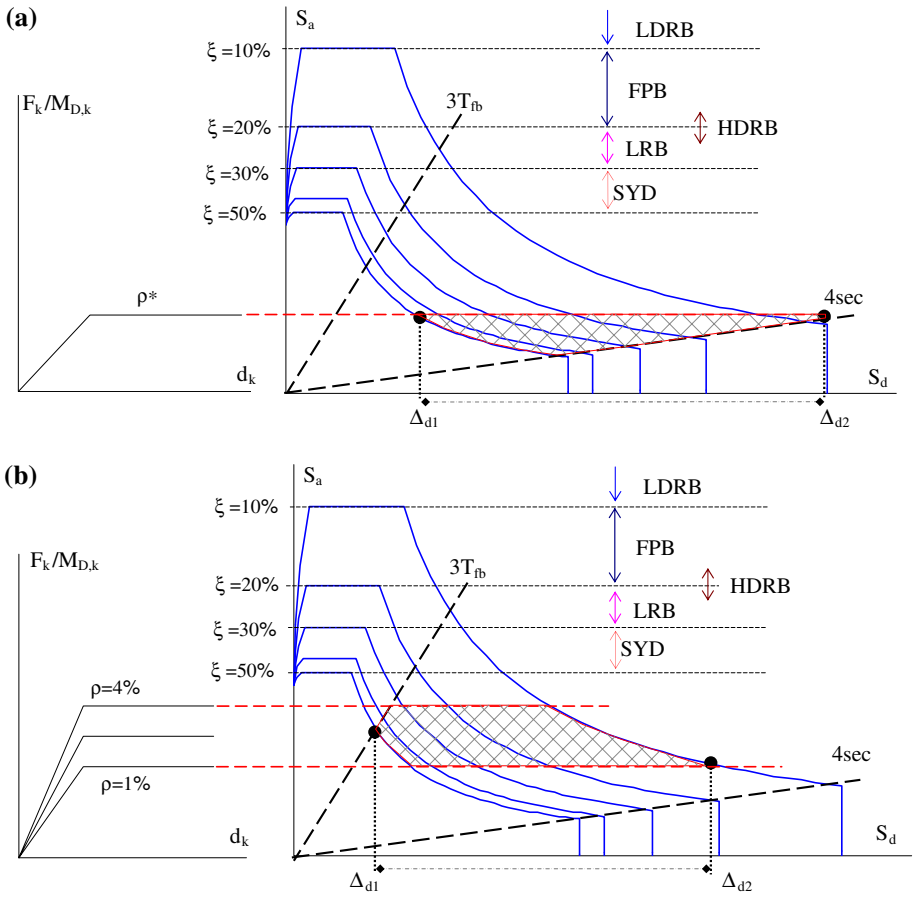

Fig. 5 Preliminary selection of IS type, design displacement and pier reinforcement ratio for the (**a**) retrofit of existing bridges and (**b**) design of new bridges

The dashed lines passing through the origin of the axis correspond to two limit values of the effective period of vibration of the bridge with seismic isolation, equal to $3T_{\mathrm{fb}}$ and 4 s, respectively, T_{fb} being the fundamental period of vibration of the bridge w/o seismic isolation. The first limit (i.e. $3T_{\mathrm{fb}}$) corresponds to the minimum value normally accepted (e.g. see (Zhang 2003)) in order to start to appreciate the beneficial effects of the longer period of vibration of the isolated structure. The second limit (i.e. 4 s) corresponds to the corner period of the constant displacement branch of the modified response spectrum adopted within the DDBD method (Priestley et al. 2007). The interceptions of such radial lines with the response spectra at 10% and 50% damping, define a preliminary range of possible design displacements.

On the left hand side of the ADRS diagram of Fig. 5 there is reported the displacement vs. acceleration ($F_{\mathrm{k}}/M_{\mathrm{D,k}}$) relationship of the most critical (lowest shear/flexural strength) pier of the bridge, in the considered direction. For existing bridges, the most critical pier is characterized by a given reinforcement ratio (ρ^*). For new bridges, a range of possible reinforcement ratios ($1\% < \rho < 4\%$) is taken into account. Considering that an elastic response

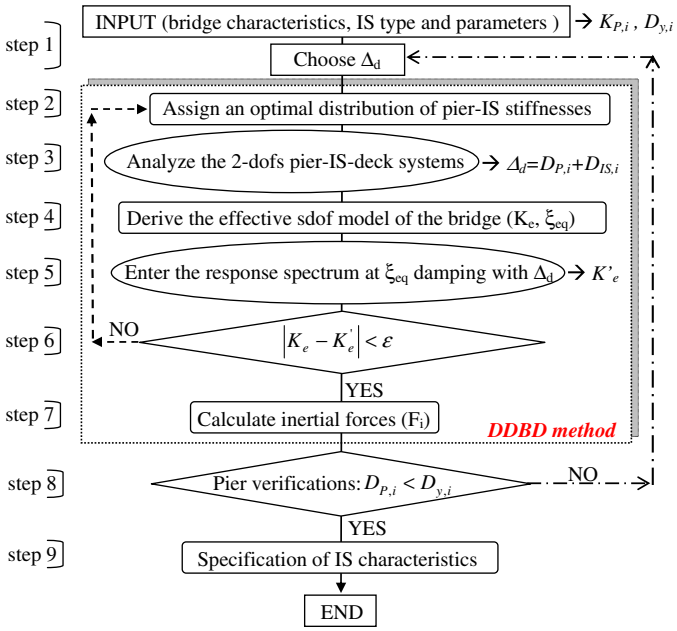

Fig. 6 Flowchart of the DDBD procedure for the retrofit of existing bridges with seismic isolation

of all the piers is required, only the performance points which fall inside the painted background of the ADRS diagrams can be preliminarily selected. Once this selection is made, an optimal IS type, design displacement (and reinforcement ratio) are identified. Obviously, the more the selected performance point is far from the boundaries of the domain the more the accurate design procedure will rapidly converge to a suitable solution.

Figure 6 shows the flowchart of the procedure for the retrofit of existing bridges with seismic isolation. The procedure illustrated in Fig. 6 is valid for both continuous and multi-span bridges, with the main difference that, for continuous bridges, reference is made to the entire deck while, for multi-span bridges, the procedure is applied separately to each span.

The first step is to define the input data of the procedure, which include bridge geometry, pier dimensions, masses, pier reinforcement ratios, etc. For what concerns the elastic stiffness and yield displacement of the piers ($D_{y,i}$), reference is made to the approach suggested by Priestley et al. (2007) based on extensive experimental results, according to which the elastic stiffness of cracked concrete sections is essentially proportional to strength and the yield displacement is constant and independent from strength. More precisely, the elastic stiffness is computed as a function of the axial load ratio and longitudinal reinforcement ratio of each pier, through the dimensionless graphs provided in (Priestley et al. 2007). Similarly, the yield displacement is evaluated as a function of the pier geometry and steel yield strain, though the expressions provided to this regard by Priestley et al. (2007). In the evaluation of $D_{y,i}$, the risk of premature shear failures are taken into account. Step 1 also includes the selection of the IS type and design displacement of the deck, based on the preliminary design procedure of Fig. 5.

The second step consists in assigning a trial optimal distribution of pier-IS stiffnesses, which guarantees a uniform rigid translation of the deck in the transverse direction. The optimal stiffness distribution is determined by centering the centre of stiffness of the pier-IS

systems with respect to the centre of mass of the bridge. To this end, a stiffness distribution proportional to the tributary masses at the deck supports is assumed.

In the first cycle of iteration the mass of the piers is neglected. In the following cycles, the analysis is repeated referring to the effective masses of the pier-IS-deck systems (m_i^*). These latter are evaluated in step 3, by examining the 2-dof systems described in Fig. 2c. The modal analysis of the 2-dof systems also indicates the contributions of each pier and IS to the design displacement of the deck (i.e. $\Delta_d = D_{P,i} + D_{IS,i}$).

In step 4 the nonlinear MDOF model of the bridge is converted into an equivalent SDOF model. Each pier-IS system is examined first, deriving the associated equivalent stiffness ($K_{eq,i}$) and equivalent damping ($\beta_{eq,i}$) by means of the following equations:

$$\frac{1}{K_{eq,i}} = \frac{1}{K_{P,i}} + \frac{1}{K_{IS,i}} \tag{6}$$

$$\beta_{eq,i} = \frac{D_{P,i} \cdot \xi_{P,i} + D_{IS,i} \cdot \xi_{IS,i}}{D_{P,i} + D_{IS,i}} \tag{7}$$

where $K_{P,i}$, $\xi_{P,i}$, $D_{P,i}$ are the elastic stiffness, equivalent viscous damping and maximum displacement of the i-th pier, respectively; $K_{IS,i}$ and $\xi_{IS,i}$ the effective stiffness and effective damping (see Fig. 4) of the corresponding IS at its maximum displacement $D_{IS,i}$.

The effective stiffness of the equivalent SDOF model of the whole bridge (or single span for multi-span bridges) is obtained by summing, in parallel, the equivalent stiffness values of each pier-IS system (i.e. $K_e = \sum K_{eq,i}$). The equivalent damping of the SDOF system is derived by combining the contributions of each pies-IS system weighted with their effective mass (i.e. $\xi_{eq} = \sum \left(m_i^* \cdot \beta_{eq,i}\right) / \sum m_i^*$).

With the target displacement Δ_d of the SDOF system derived from Eq. 1, the displacement response spectrum at ξ_{eq} is entered to determine the effective period of the SDOF system (see Fig. 1c). A new value of global effective stiffness (K'_e) is thus obtained and compared to the previous one of step 2. If they differ more than a given tolerance (i.e. if $|K'_e - K_e| > 0.01$), the effective stiffnesses of the IS's ($K_{IS,i}$) are revised according to K'_e and steps 2–5 repeated until convergence is reached. At the end of the iterative process, preliminary pier verifications are carried out, based on the maximum displacements provided by the analysis ($D_{P,i} < D_{y,i}$). If pier verifications are not satisfied, a new design displacement is selected and steps 2–8 repeated. In the last step of the design procedure (step 9 in Fig. 6) the mechanical characteristics of each IS are fully specified, based on their equivalent linear maximum response and the mechanical parameters (e.g. friction coefficient, post-yield hardening ratio, viscous damping) assumed at the beginning of the analysis.

With the inertial forces F_i derived in step 7 (see Eq. 4), a linear static analysis is performed, modeling the IS's though their effective stiffnesses, in order to determine the stress distributions in all the structural members, including shear forces and overturning moments transmitted to the foundations.

In any case, a final verification through (nonlinear) time-history analysis is always recommended.

Figure 7 shows the flowchart of the procedure for the design of new bridges with seismic isolation. It is practically the same as that valid for the retrofit of existing bridges (see Fig. 6), except for the pier reinforcement ratios which are still unknown at the beginning of the analysis.

A trial value of reinforcement ratio is then adopted in step 2, in order to determine the elastic stiffness of the piers. At the end of the analysis (step 4 in Fig. 7), the maximum ratio between maximum and yield displacements of the piers is checked. If it differs significantly

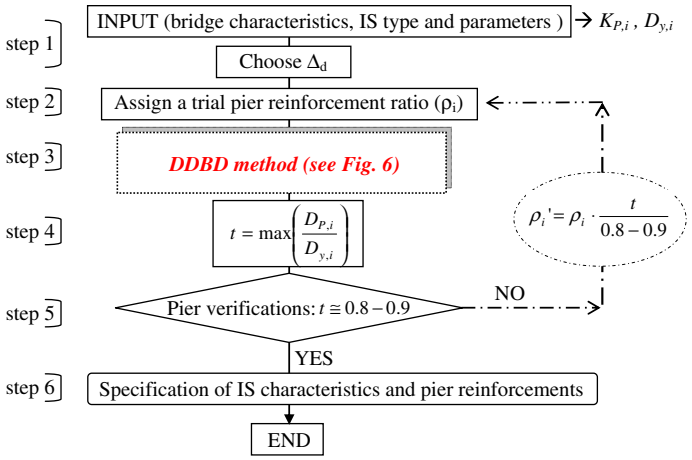

Fig. 7 Flowchart of the DDBD procedure for the design of new bridges with seismic isolation

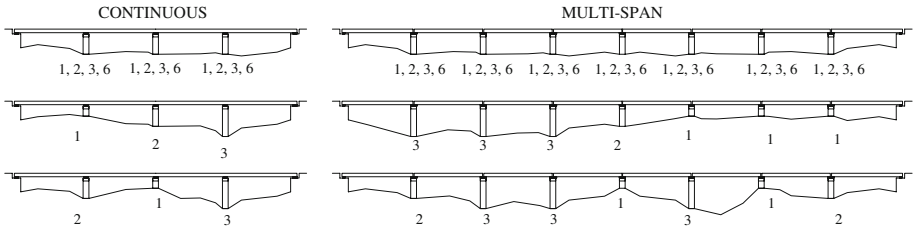

Fig. 8 Bridge configurations

from a given threshold value (e.g. 0.8–0.9), which takes into account possible overstrength of the IS, the pier reinforcement ratios are properly revised and a new cycle of analysis is performed.

As said before, the proposed procedure provides the mechanical characteristics (stiffness, damping, displacement capacity, strength, etc) of each IS, which satisfy the selected design performance objectives (see paragraph 2.1), separately in the longitudinal and transverse direction of the bridge. In principle, these characteristics will result different from one IS to another, especially for irregular bridges with piers of different heights. Nevertheless, a reduction to 1–2 different IS types is needed at the end of the design process, in order to guarantee the applicability of the seismic isolation and limit the related costs.

3 Nonlinear time-history analyses

Some validation studies through nonlinear time-history analyses (NTHA) have been carried out, on three different configurations of continuous and multi-span bridges, in order to assess the reliability of the proposed DDBD procedure. The bridge configurations examined in this study are shown in Fig. 8.

The continuous bridges have four 35 m spans, the multi-span bridges have eight 35 m spans. All the bridges have a steel deck with a box cross section of 6.88 m^2, a moment of

inertia for bending around the vertical axis of 87.24 m^4 and a weight per unit of length of approximately 200 kN/m.

The deck is supported by RC piers characterized by a rectangular hollow cross section of 4 m height by 2 m width and 0.4 m thickness. The piers have a weight per length unit of 104 kN/m. The longitudinal reinforcement ratio of the piers is equal to 1%. The transverse reinforcement of the piers consists of 12 mm diameter hoops at 100 mm spacing. All the piers have a pier cap of 1 m height and 500 kN weight. The resistances of concrete and steel are equal to 39 and 462 Mpa, respectively.

One regular and two irregular layout of pier heights have been considered for both continuous and multi-span bridges (see Fig. 8). Basically, they are very similar to those considered in previous studies (Casarotti and Pinho 2007; Priestley et al. 1996). The main difference is related to the pier height, which has been taken equal to a multiple (1, 2 and 3, precisely) of 4 m, instead of 7 m. For regular bridges, an additional pier height of 24 m (i.e. 6 times the basic height of 4 m) has been considered. The aforesaid selection has been purposely done in order to assess the reliability of the proposed DDBD procedure for a number of different bridge configurations, including that of bridges with piers of 4 m height (i.e. a very favourable configuration for the application of seismic isolation) and that of bridges with piers of 24 m height (i.e. a critical configuration for the application of seismic isolation, due to the high flexural deformability of the piers, comparable to that of the isolation system). The total number of bridges examined is 12, as shown in Fig. 8, where the label numbers 1, 2, 3 and 6 correspond to pier heights of 4, 8, 12 and 24 m, respectively. The fundamental period of vibration of the pier-deck systems w/o IS are 0.1, 0.3, 0.6 and 1.6 s, respectively.

Numerical simulation analyses have been carried out with SAP2000_Nonlinear (Computers and Structures Inc 2002). The piers have been modeled through linear beam-column elements with a global (flexural+shear) stiffness equal to the elastic stiffness considered in the design procedure. A 5% viscous damping has been assigned to the RC piers. The deck has been modeled through linear beam-column elements characterized by a Young and shear modules of 25,000 and 10,000 MPa, respectively. Nonlinear link elements have been used to reproduce the cyclic force-displacement behaviour of the isolation systems.

Two different IS types have been examined, namely: visco-elastic systems (see Fig. 3a) with damping ratio equal to 10, 20 and 30% and elasto-plastic systems (see Fig. 3b) with post-yield hardening ratio of 5, 10 and 15% and maximum ductility of 20. A target displacement (Δ_d) of 270 mm has been always assumed in the design procedure.

A set of seven natural and artificial ground acceleration-time histories (see Fig. 9a), compatible (on average) with a DBD-adapted version of the displacement response spectrum provided by Eurocode 8 (CEN 1998) for soil type C, has been used in the numerical simulation analyses. Actually, the only difference with respect to the standard EC8-soil C spectrum consists in the corner period T_D, corresponding to the transition from the velocity-sensitive to the displacement-sensitive region of the spectrum, which is taken equal to 4 s instead of 2.5 s. Reference has been made to a peak ground acceleration (PGA) of $S \cdot 0.35$ g, S being the soil amplification factor, equal to 1.15 for the selected ground type.

In Fig. 9b the design response spectrum adopted in the DDBD procedure is compared to the average response spectrum associated to the selected accelerograms. As can be seen, some differences are observed, especially in the period range of more interest for seismically isolated structures (i.e. between 2 and 3 s). In order to avoid any influence of such spectral discrepancies on the evaluation of the accuracy of the proposed design procedure, the PGA of the ground acceleration-time histories has been adjusted in such a way as to get the coincidence between design and average displacement response spectrum at the effective period of vibration of the isolated structure.

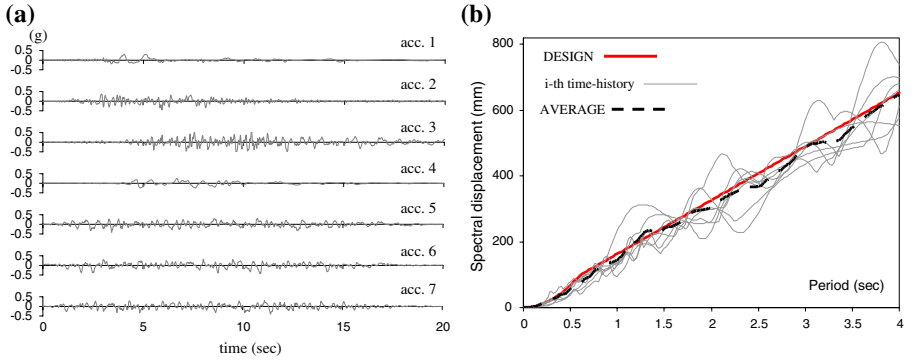

Fig. 9 (**a**) Ground acceleration-time histories employed in the numerical simulation analyses and (**a**) comparison between the design response spectrum and the average response spectrum associated to the selected accelerograms

The results of NTHA are presented in terms of (i) displacement profile of the deck at the maximum absolute displacement, (ii) maximum top displacements of piers and (iii) maximum pier base moments. For brevity, the attention is focused on the transverse response of the bridge only, which is generally the most difficult to control, especially for bridges with a great variability of pier heights.

In Tables 1–4, the most important results of NTHA are compared to the predictions of the DDBD method. Tables 1 and 2, in particular, refer to four different configurations of continuous (C) bridges, equipped with different visco-elastic (VE) and elasto-plastic (EP) IS's, respectively. Similarly, in Tables 3 and 4 the results relevant to four different configurations of multi-span (MS) bridges are examined. Bridge configuration, IS characteristics and design displacements are identified in the first three columns of Tables 1–4. In the following two columns, the expected effective period of vibration of the SDOF system and equivalent damping ratio of each bridge configuration are specified. The percent differences between the design displacement of the deck (Δ_d) and the average maximum deck displacement derived from NTHA ($D_{D,max}$) are listed in the column labeled with ΔD. Negative values of ΔD mean that

Table 1 Comparison between numerical results and design objectives for continuous bridges with visco-elastic IS's

Bridge Config.	IS damping (%)	Δ_d (mm)	T_e (s)	ξ_{eq} (%)	$D_{D,max}$ (mm)	ΔD (%)	θ_{max} (deg)	$\frac{D_{P-SAP}}{D_{P-DDBD}}$	$\frac{M_{P-SAP}}{M_{P-DDBD}}$
C111	10	270	2.03	10.0	259	−4	5.71E-07	0.98	0.98
	20	270	2.62	20.0	267	−1	6.67E-07	1.16	1.15
	30	270	3.09	30.0	236	−13	5.71E-07	1.23	1.17
	10	270	1.8	6.8	274	1	2.00E-04	1.07	1.05
C666	20	270	2.31	14.4	276	2	9.49E-05	1.15	1.14
	30	270	2.83	24.2	278	3	9.71E-05	1.35	1.33
								1.15	1.13
C123	20	270	2.61	19.8	268	−1	5.40E-05	1.18	1.17
								1.23	1.22
								1.18	1.16
C213	20	270	2.61	19.8	267	−1	3.63E-05	1.15	1.14
								1.23	1.21

Table 2 Comparison between numerical results and design objectives for continuous bridges with elasto-plastic IS's

Bridge Config.	IS hardening ratio (%)	Δ_d (mm)	T_e (s)	ξ_{eq} (%)	$D_{D,max}$ (mm)	ΔD (%)	θ_{max} (deg)	$\frac{D_{P-SAP}}{D_{P-DDBD}}$	$\frac{M_{P-SAP}}{M_{P-DDBD}}$
C111	5	270	3.07	29.5	255	−6	3.86E-07	1.06	1.03
	10	270	2.55	18.8	270	0	5.71E-07	1.02	1.01
	15	270	2.24	13.4	235	−13	3.86E-07	0.90	0.90
	5	270	2.94	26.6	256	−5	1.46E-04	1.31	1.30
C666	10	270	2.48	17.4	271	0	1.34E-04	1.10	1.11
	15	270	2.21	12.9	254	−6	8.80E-05	0.99	0.99
								1.10	1.09
C123	10	270	2.55	18.7	274	1	9.71E-05	1.13	1.09
								1.18	1.15
								1.13	1.09
C213	10	270	2.55	18.7	273	1	6.60E-05	1.10	1.09
								1.18	1.15

Table 3 Comparison between numerical results and design objectives for multi-span bridges with visco-elastic IS's

Bridge Config.	IS damping (%)	Δ_d (mm)	T_e (s)	ξ_{eq} (%)	$D_{D,max}$ (mm)	ΔD (%)	θ_{max} (deg)	$\frac{D_{P-SAP}}{D_{P-DDBD}}$	$\frac{M_{P-SAP}}{M_{P-DDBD}}$
MS 1111111	10	270	2.03	10.0	259	−4	1.03E-05	0.97	0.97
	20	270	2.62	20.0	263	−3	1.06E-05	1.13	1.14
	30	270	3.10	30.0	236	−13	9.71E-06	1.21	1.16
MS 6666666	10	270	2.00	9.5	265	−2	2.16E-03	1.04	1.02
	20	270	2.46	17.0	283	5	1.87E-03	1.13	1.12
	30	270	2.91	25.9	293	9	1.99E-03	1.34	1.31
								1.22	1.21
MS 3332111	20	270	2.61	19.8	272	1	1.97E-04	1.17	1.16
								1.14	1.13
								1.17	1.16
MS 2331312	20	270	2.61	19.8	272	1	1.89E-04	1.22	1.21
								1.14	1.13

the maximum displacement provided by NTHA underestimates the design displacement and therefore the DDBD method is conservative.

The maximum rotation of the deck (θ_{max}) is also reported in Tables 1–4. Obviously, for multi-span bridges, reference is made to single spans. Finally, in the last two columns of Tables 1–4, the maximum pier displacement and pier base moment ratios (NTHA results vs. DDBD prediction) are reported.

Contrasting conclusions can be drawn from Tables 1–4. On the one hand, the DDBD procedure tends to overestimate a little the maximum deck displacement and maximum IS displacements (not shown in Tables 1–4), leading to errors, however, always lower than 15%, even when the piers contribute significantly with their deformability to the target displacement of the deck (ref. C666 bridge configuration). On the other hand, the DDBD procedure tends to underestimate the maximum pier displacements and the corresponding maximum

Table 4 Comparison between numerical results and design objectives for multi-span bridges with elasto-plastic IS's

Bridge Config.	IS hardening ratio (%)	Δ_d (mm)	T_e (s)	ξ_{eq} (%)	$D_{D,max}$ (mm)	ΔD (%)	θ_{max} (deg)	$\frac{D_{P-SAP}}{D_{P-DDBD}}$	$\frac{M_{P-SAP}}{M_{P-DDBD}}$
MS 1111111	5	270	3.07	29.5	255	−6	1.40E-05	1.05	1.03
	10	270	2.55	18.8	271	0	6.86E-06	1.02	0.99
	15	270	2.24	13.4	235	−13	8.57E-06	0.89	0.90
MS 6666666	5	270	2.97	27.2	255	−6	9.68E-04	1.30	1.28
	10	270	2.55	18.7	272	1	8.57E-04	1.09	1.11
	15	270	2.32	14.7	252	−7	1.19E-03	0.98	0.99
								1.17	1.14
MS 3332111	10	270	2.55	18.8	273	1	2.22E-04	1.12	1.10
								1.09	1.08
								1.12	1.10
MS 2331312	10	270	2.55	18.8	273	1	2.06E-04	1.17	1.14
								1.09	1.08

shear forces and base bending moments. The errors increase while increasing the damping level of the IS (see VE-30% and EP-5%), although they generally do not exceed 25%. The same trend is observed also for the analysis cases not shown in Tables 1–4. In accordance with the results recently reported by other authors (Priestley et al. 2007), the above said discrepancies can be probably ascribed to the inaccuracy of the used Damping Reduction Factor (DRF). In the proposed design procedure, indeed, the DRF of EC8 (i.e. $\eta = \sqrt{10/(5+\xi)}$) has been employed to derive high damping response spectra. Possible improvements in the accuracy of the method may derive from the use of different relationships. To substantiate this hypothesis, a number of preliminary verifications have been conducted on the bridge C333. In particular, the VE system at 30% and the EP system at 5% have been re-designed using the DRF adopted in the old Italian guidelines (SSN 1998) for the design, construction and testing of seismically isolated structures (i.e. $\eta = \sqrt[3]{7/(2+\xi)}$). NTHA have been then repeated and the results compared to the design predictions. The errors in terms of maximum pier displacements and maximum bending moments have been found to reduce from 23–25% to 10–12% for the VE system and from about 15–16% to just 1–2% for the EP system, without significant loss of accuracy in the attainment of the target displacement profile of the deck. Obviously, further studies are needed to fully prove the consistency of the previous observation and get enhanced formulations of the damping reduction factor, probably specialized to each IS type.

It can be observed, from Tables 1–4, that the rotation of the deck is always negligible for both continuous and multi-span bridges. This is confirmed by the examination of the bridge response under single earthquakes, shown in Fig. 10 for regular continuous bridges differing in the pier heights (C111 and C666, respectively), in Fig. 11 for irregular bridges equipped with different IS types (VE with 20% viscous damping ratio and EP with 10% hardening ratio), and finally in Fig. 12 for different configurations of multi-span bridges (MS3333333, MS3332111 and MS2331312, respectively).

The comparison of the displacement-time histories of the ends of the deck (Figs. 10b–11b), or of the ends of the first span (Fig. 12b), confirms that they are perfectly superimposed for

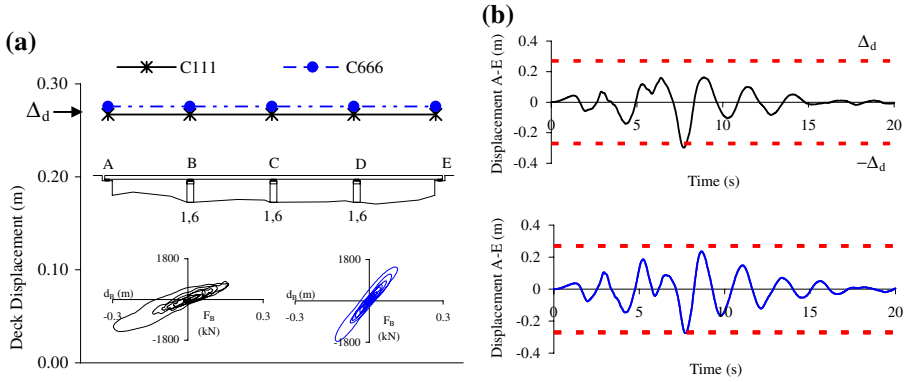

Fig. 10 Bridges C111 and C666 equipped with visco-elastic IS with 20% damping ratio. Seismic response due to the accelerogram n. 2: (**a**) displacement profile of the deck at the maximum absolute displacement and force-displacement cyclic behaviour of the IS placed on pier B; (**b**) displacement-time histories of the ends of the deck (points A and E)

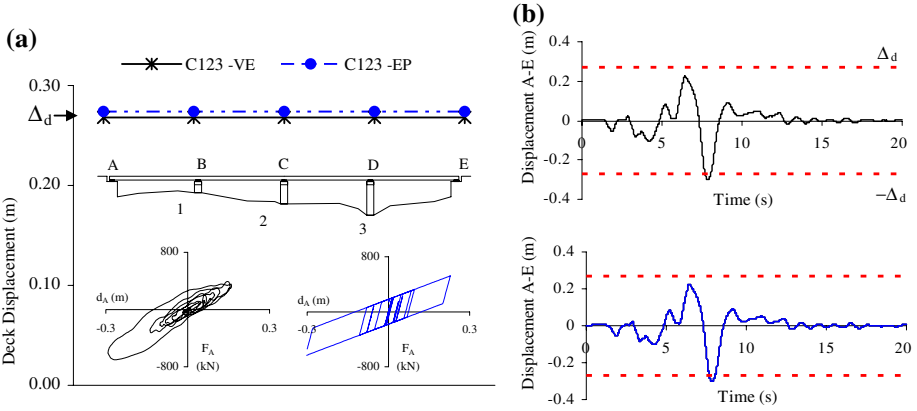

Fig. 11 Bridge C123 equipped with visco-elastic IS with 20% damping ratio and elasto-plastic IS with 10% post-yield hardening ratio. Seismic response due to the accelerogram n. 2: (**a**) displacement profile of the deck at the maximum absolute displacement and force-displacement cyclic behaviour of the IS placed on abutment A; (**b**) displacement-time histories of the ends of the deck (points A and E)

the entire duration of the seismic response of the bridge, regardless the bridge configuration, the IS type and the ground motion characteristics taken into consideration.

The force-displacement diagrams shown in Figs. 10a and 11a point out the influence of the pier deformability on the IS response (Fig. 10a) and the differences in terms of cyclic behaviour between VE-IS and EP-IS exhibiting the same level of effective damping (Fig. 11a).

In Fig. 13, the ratios between the (average) maximum pier displacements ($D_{P,max}$), derived from NTHA, and the corresponding yield displacements (D_y), calculated following the approach of Priestley et al. (2007), are shown. Results are reported for different configurations of regular continuous bridges, equipped with VE-IS with 10–20–30% viscous damping (Fig. 13a) and EP-IS with 5–10–15% hardening ratio (Fig. 13b). As expected, the displacement ratios increase while increasing pier heights and while decreasing the effective damping of the IS. For all the examined cases, however, the displacement ratios remain

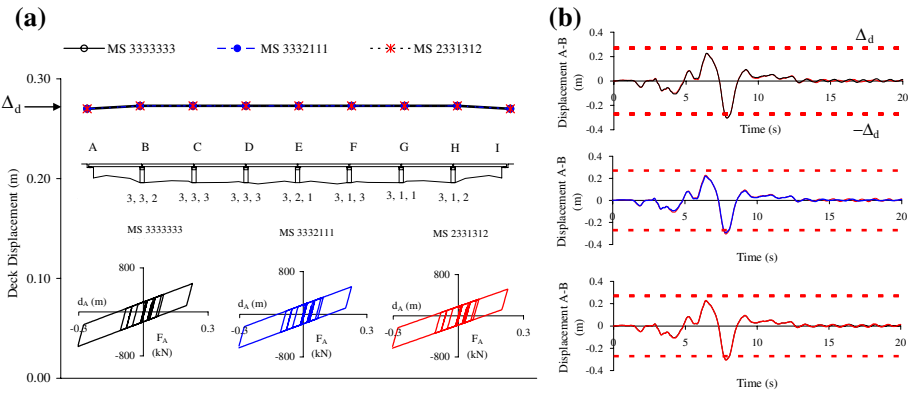

Fig. 12 Bridges MS3333333, MS3332111 and MS2331312 with elasto-plastic IS with 10% post-yield hardening ratio. Seismic response due to the accelerograms n. 2: (**a**) displacement profile of the deck at the maximum absolute displacement and force-displacement cyclic behaviour of the IS placed on abutment A; (**b**) displacement-time histories of the ends of the first span (points A and B)

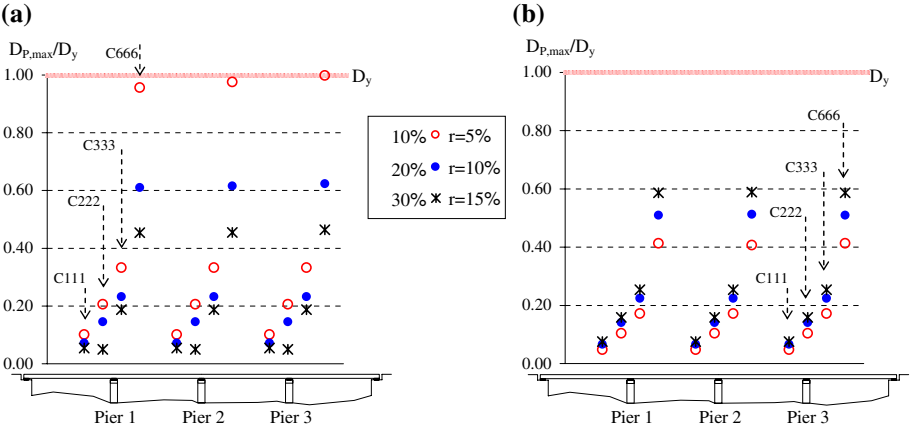

Fig. 13 Comparison between maximum top displacement and yield displacement of the piers for regular continuous bridges equipped with (**a**) visco-elastic and (**b**) elasto-plastic IS's

significantly lower than 1, except for the bridge configuration C666 with VE-IS having 10% viscous damping, for which the maximum pier displacements is comparable to their elastic limit. The large margins with respect to $D_{y,i}$ are mainly due to fact that the selection of Δ_d has not been particularized to each analysis case but derived for the most critical case only (C666 with VE-10%, precisely), based on the preliminary design approach described in Fig. 5a.

To conclude, the aforesaid observations clearly prove that the proposed design procedure is able to attain the desired uniform target displacement of the deck, limiting the maximum pier displacements below their elastic limit, thus fully realizing the performance objective of the design.

4 Conclusions

A Direct Displacement-Based Design (DDBD) methodology for continuous and multi-span bridges with different Isolation Systems (IS's) has been presented. Four different force-displacement models of IS have been considered, which can be used to describe the cyclic behaviours of a wide variety of IS's, including: (i) High Damping Rubber Bearings, (ii) Lead Rubber Bearings, (iii) Friction Pendulum Bearings and (iv) combinations of Flat Sliding Bearings with different auxiliary devices.

The design procedure has been applied to a series of 4-span continuous bridges and 8-span simply supported bridges, characterized by either regular or irregular layout of pier heights, considering two different IS types, namely: visco-elastic systems with damping ratio equal to 10, 20 and 30% and elasto-plastic systems with post-yield hardening ratio of 5, 10 and 15%. The prediction of the DDBD method have been compared to the results of nonlinear time-history analyses (NTHA), carried out with SAP2000, using a set of seven spectrum-compatible accelerograms.

The results of NTHA prove that bridges designed according to the proposed DDBD procedure achieve the desired target displacement profile with piers that remain elastic. Based on the results of NTHA, possible refinements to the method have been also identified. They include an improved formulation of the damping reduction factor, probably specialized to each IS type.

The proposed design procedure is not intended to cover all the aspects related to the design of bridges with seismic isolation. Basically, it establishes, in detail, all the fundamental steps for the practical application of the DDBD approach to seismically isolated bridges. Further developments and refinements are still needed. For instance, an optimization routine, to be used in the post design stage, for dimensioning the IS's taking into account a series of practical aspects, such as limitation of different IS devices/components, optimization of the bridge response in the two directions (transverse and longitudinal), partially isolated bridges, etc., would be very useful to make the proposed DDBD procedure really attractive in practical design.

Acknowledgements This work has been carried out within the RELUIS 2005-2008 program, Project No. 4, funded by the Italian Civil Protection Department.

References

Al-Hussaini TM, Zayas VA, Constantinou MC (1994) Seismic isolation of a multi-story frame structure using spherical sliding isolation systems, Technical Report No. NCEER-94-0007, National Center for Earthquake Engineering Research, Buffalo, NY

Bertero RD, Bertero VV (2002) Performance-based seismic engineering: the need for a reliable conceptual comprehensive approach. Earthquake Eng Struct Dyn 31(3):627–652

Calvi GM, Pavese A (1997) Conceptual design of isolation systems for bridge structures. J Earthquake Eng 1(1):193–218

Casarotti C, Pinho R (2007) An adaptive capacity spectrum method for assessment of bridges subjected to earthquake action. Bull Earthquake Eng 5(3):377–390

CEN ENV-1-1 European Committee for Standardisation (1998) Eurocode 8: design provisions for earthquake resistance of structures, Part 1.1: General rules, seismic actions and rules for buildings

Chopra AK (1997) Dynamics of structures: theory and application to earthquake engineering. Prentice-Hall Ltd

Computers and Structures Inc (2002) SAP2000 Analysis Ref. Manual, Version 8.0, Berkeley, CA

Constantinou MC, Symans MD, Tsopelas P, Taylor DP (1993) Fluid viscous dampers in applications of seismic energy dissipation and seismic isolation. In: Proceedings of ATC-17-1 seminar on seismic isolation, passive energy dissipation, and active control; San Francisco, CA, pp 581–591

Derham CJ, Kelly JM, Thomas AG (1985) Nonlinear natural rubber bearings for seismic isolation. Nuc Eng Design 84(3):417–428

Dolce M, Cardone D, Marnetto R (2000) Implementation and testing of passive control devices based on shape memory alloys. Earth Eng Struct Dyn (29):945–958

Dolce M, Cardone D, Croatto F (2005) Frictional behaviour of steel-PTFE interfaces for seismic isolation. Bull Earthquake Eng 3(1):75–99

Dolce M, Cardone D, Ponzo FC (2007) Shaking-table tests on reinforced concrete frames with different isolation systems. Earthquake Eng Struct Dyn 36(5):573–596

Eggert H, Kauschke W (2002) Structural bearings. Ernst & Sohn, Berlin

Higashino M, Okamoto S (2006) Response control and seismic isolation of buildings. Taylor & Francis Ltd

Kelly TE (1992) Skellerup industries lead rubber isolation bearings: experimental properties. Holmes Consulting Group

Kowalsky MJ (2002) A displacement-based approach for the seismic design of continuous concrete bridges. Earth Eng Struct Dyn (31):719–747

Naeim F, Kelly JM (1999) Design of seismic isolated structures. Wiley

Pettiga D, Priestley MJN (2005) Dynamic behaviour of reinforced concrete frames designed with direct displacement-based design. J Earthquake Eng 9(SP2):309–330

Priestley MJN (1993) Myths and fallacies in earthquake engineering—conflicts between design and reality. Bull NZ Nat Soc Earthquake Eng 26(3):329–341 (12 ref)

Priestley MJN (2003) Myths and fallacies in earthquake engineering, Revisited. IUSS Press, Pavia (Italy)

Priestley MJN, Seible F, Calvi GM (1996) Seismic design and retrofit of bridges. Wiley, New York, USA, 686 pp

Priestley MJN, Calvi GM, Kowalsky MJ (2007) Displacement-based seismic design of structures. IUSS Press, Pavia, Italy, 720 pp

Shibata A, Sozen M (1976) Substitute structure method for seismic design in reinforced concrete. J Struct Div – ASCE 102(12):3548–3566

Skinner RI, Robinson H, McVerry GH (1993) An introduction to seismic isolation. Wiley

SSN (1998) Presidenza del Consiglio Superiore dei LL.PP. – Servizio Tecnico Centrale, Linee guida italiane per la progettazione, esecuzione e collaudo di strutture isolate dal sisma, Roma

Sullivan TJ, Priestley MJN, Calvi GM (2005) Development of an innovative seismic design procedure for frame-wall structures. J Earthquake Eng (9):279–307

Taylor AW, Lin AN, Martin JW (1992) Performance of elastomers in isolation bearings: a literature review. Earthquake Spectra 8(2):279–304

Zhang R (2003) Seismic isolation and supplemental energy dissipation. In: Chen WF, Duan L (eds) Bridge engineering: seismic design. CRC Press